

# TFY4200 - "LAB" 3

## Mie theory

Svein Åmdal

April 2020

### 1 Analyse code

Let from now on BH = Bohren & Huffman[2].

---

```
% ../expcoeff/expcoeff_mie.m lines 26-36

%% Calculate auxiliary parameters
Sx = ricbesj(n, x);
dSx = dricbesj(n, x);
Smx = ricbesj(n, m*x);
dSmx = dricbesj(n, m*x);
xix = ricbesh(n, x);
dxix = dricbesh(n, x);

%% Calculate expansion coefficients
an = (m*Smx.*dSx - Sx.*dSmx) ./ (m*Smx.*dxix - xix.*dSmx);
bn = (Smx.*dSx - m*Sx.*dSmx) ./ (Smx.*dxix - m*xix.*dSmx);
```

---

The final expressions correspond to BH eq. (4.56) and (4.57), and are the final scattering wave expansion coefficients. They assume the permeabilities of the particle and surroundings are equal, and are written in terms of the Riccati-Bessel functions and their derivatives, which are called above.

In adjacent folders are similar expressions for cylinder particles, and stratified cylinder and sphere particles, although I have not found these in BH. One example of the definitions of the Riccati-Bessel function family is given:

---

```
% ../bessel/dricbesj.m

function [S] = dricbesj(nu,z)

S = 0.5*sqrt(pi/2/z)*besselj(nu+0.5,z) + sqrt(pi*z/2)*dbesselj(nu+0.5,z);

end
```

---

This describes the derivative of the Riccati-Bessel function of the first kind, which in BH is called  $\psi_n$  and is defined right above eq. (4.56). The expansion coefficients are for instance used to calculate cross sections of scattering.

---

```
% ../util/asmmie.m lines 38-47

%% Calculate amplitude scattering matrix
S = zeros(2,2,nang);
S(1,1,:) = anEn*taun + bnEn*pin;
```

---

```

S(2,2,:) = anEn*pin + bnEn*taun;

%% Calculate cross sections
C.ext = 2*pi/k^2*sum(n2.*real(an + bn));
C.sca = 2*pi/k^2*sum(n2.*(abs(an).^2 + abs(bn).^2));
C.abs = C.ext - C.sca;
C.k = k;

```

---

S corresponds to BH eq. (4.74), while  $C_{\text{sca}}$  and  $C_{\text{ext}}$  corresponds to BH eqs. (4.61) and (4.62). The code also writes something I can only assume to be an expanded version of BH eq. (4.77), namely the Müller matrix given by:

---

```

% ../util/getMuellerMatrix.m

function [ M ] = getMuellerMatrix( S )

M = zeros([4, 4, size(S(1,1,:))]);

S2 = S(1,1,:);
S4 = S(1,2,:);
S3 = S(2,1,:);
S1 = S(2,2,:);
S1abs = abs(S1).^2;
S2abs = abs(S2).^2;
S3abs = abs(S3).^2;
S4abs = abs(S4).^2;

M(1,1,:) = 0.5*(S1abs + S2abs + S3abs + S4abs);
M(1,2,:) = 0.5*(-S1abs + S2abs - S3abs + S4abs);
M(1,3,:) = real(S2.*conj(S3) + S1.*conj(S4));
M(1,4,:) = imag(S2.*conj(S3) - S1.*conj(S4));
M(2,1,:) = 0.5*(-S1abs + S2abs + S3abs - S4abs);
M(2,2,:) = 0.5*(S1abs + S2abs - S3abs - S4abs);
M(2,3,:) = real(S2.*conj(S3) - S1.*conj(S4));
M(2,4,:) = imag(S2.*conj(S3) + S1.*conj(S4));
M(3,1,:) = real(S2.*conj(S4) + S1.*conj(S3));
M(3,2,:) = real(S2.*conj(S4) - S1.*conj(S3));
M(3,3,:) = real(S1.*conj(S2) + S3.*conj(S4));
M(3,4,:) = imag(S2.*conj(S1) + S4.*conj(S3));
M(4,1,:) = imag(conj(S2).*S4 + conj(S3).*S1);
M(4,2,:) = imag(conj(S2).*S4 - conj(S3).*S1);
M(4,3,:) = imag(S1.*conj(S2) - S3.*conj(S4));
M(4,4,:) = real(S1.*conj(S2) - S3.*conj(S4));

end

```

---

which is more general than the version where  $S_3$  and  $S_4$  are zero, as in BH eq. (4.77).

## 2 Test the most important functions used in the solutions

The building blocks of the expansion is the function in the Riccati-Bessel family. Three examples of the code implementation of these functions are plotted in figs. 1 to 3.

The plotted functions look like they should, so we allow ourselves to assume that all basic functions are well implemented.

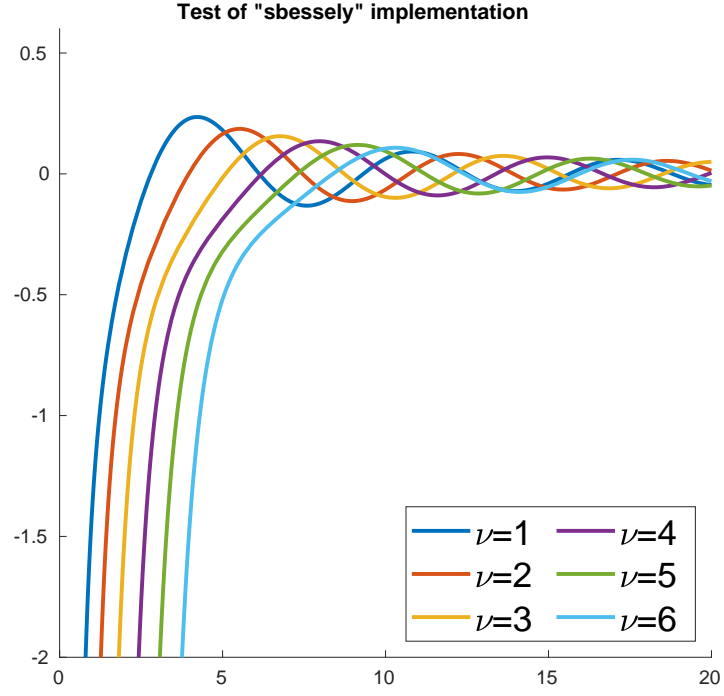


Figure 1: Implementation of the spherical Bessel function of the second kind, defined by  $y_\nu(\rho) = \sqrt{\pi/2\rho}Y_{\nu+1/2}(\rho)$ .

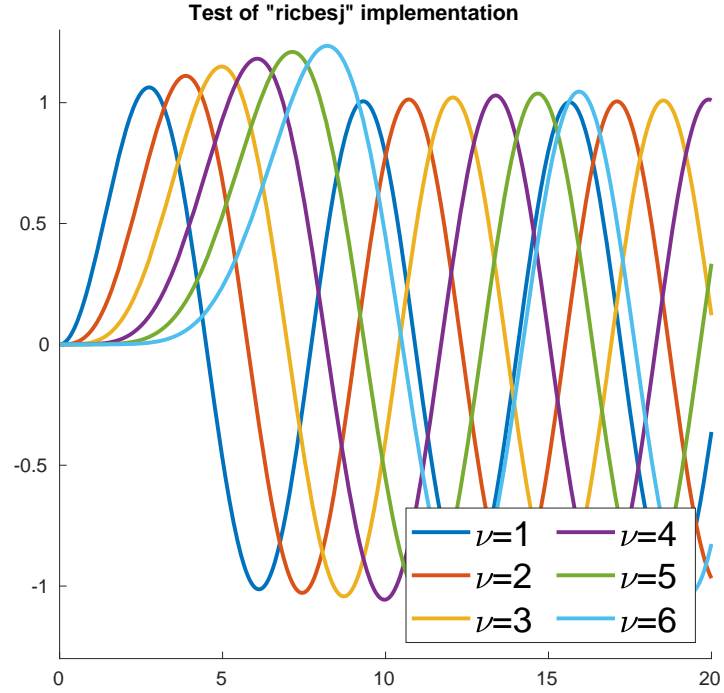


Figure 2: Implementation of the spherical Riccati-Bessel function of the first kind, defined by  $\psi_\nu(\rho) = \rho j_\nu(\rho)$ , and  $j_\nu(\rho)$  is the first-kind analog to the definition of  $y_\nu(\rho)$  in fig. 1.

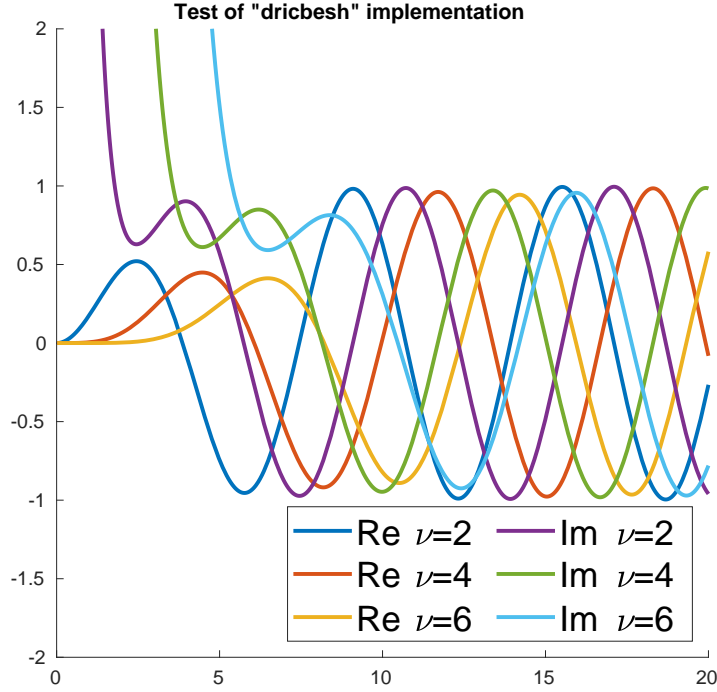


Figure 3: Implementation of the derivative of the Riccati-Hankel function of the first kind, defined by  $d\xi_\nu(\rho)/d\rho = d/d\rho [\rho h_\nu^{(1)}(\rho)]$ , and  $h_\nu^{(1)}(\rho)$  is the first kind Hankel function analog to the definition of  $y_\nu(\rho)$  in fig. 1.

### 3 Convergence tests

We will study a particular case to check how many terms in the series expansion in BH eq. (4.45) is reasonable to include. Given that the analytic solution is an infinite series, one cannot necessarily compare the truncated series with a solution in closed form. Therefore, we calculate the absolute error between an expansion with a variable  $n$  terms, and a pre-calculated expansion with a fixed (large)  $N$  terms. The open source MATLAB code uses the Wiscombe criterion[7], for truncation, and allows extension of this  $N$  by multiplying with some "convergence factor"  $c$ . So  $c = 1$  is adhering to the classical Wiscombe criterion. We set up an example with the numerical values given in BH section 4.4.5, and calculate the scattering matrix and scattering cross section when we let  $c$  vary from 0.1 to 1. This range is convenient for plotting on a logarithmic scale. We would have given the plot for a more extended range, but there are evidently some numerical stability issues for  $c$  outside this range. If  $c = 0.01$ , the program produced matrices with wrong dimensions, and if  $c = 10$ , we encounter zero-division errors. These problems may be rectified with increasing the floating point precision of the data. The absolute errors in the related quantities between using the number of terms suggested by the Wiscombe criterion, and the same number multiplied by a  $c$  in the range between 0.1 and 1, summed across 180 discretised angles, is given in [1].

By this, we conclude (at least in the given range), that both types of error become very small close to  $c = 1$ , and given that the terms in the expansion are strictly decreasing, the error from the remaining terms is very small, probably no greater than  $10^{10}$ . We regard the regular ( $c = 1$ ) convergence criterion as valid.

(I must admit, however, that this test is somewhat flawed. There is no other way to change the number of terms in truncated series without altering the source code, which is something I don't want to do.)

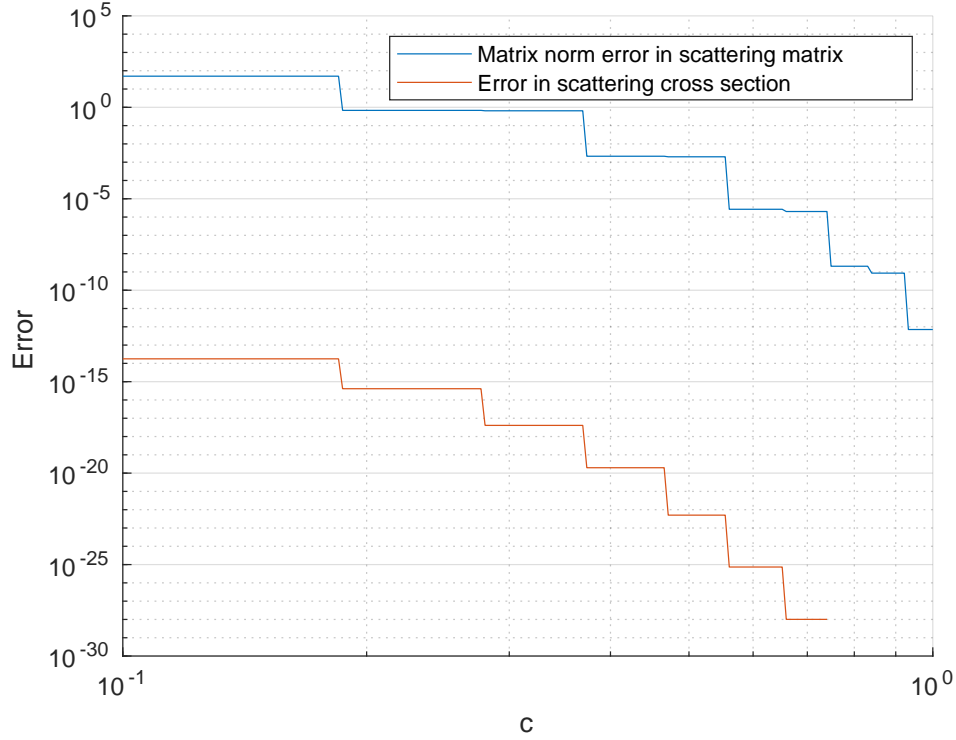


Figure 4: The absolute error between choosing a series truncation in accordance with the Wiscombe criterion, or truncated a factor  $c$  terms before that, summed over all 180 (discretised) scattering angles, for two different products of the Mie numerics; the matrix norm of the scattering matrix, and the error in total scattering cross section.

## 4 Simulation of extinction efficiency and scattering

Taking the parameters suggested in BH 11.2.1, all we need is a function for the refractive index of MgO. To make the function explicit, we use the function suggested by Stephens and Malitson[5]. The extinction efficiency calculated for MgO is shown in section 4.

Similarly for water, using the refractive index from IAPWS[6], the extinction efficiency is shown in section 4.

Unfortunately, I don't think either of these plots look too similar to the plots presented in BH. To calculate the scattering matrix for some different size parameters  $x = ka$ , I still needed to select some specific values for the Mie calculation. Selecting  $a = 1e - 6$ , and letting  $\lambda$  vary accordingly, the absolute value of the (otherwise complex) (1, 1)- and (2, 2)-components of the scattering matrix is shown in section 4.

In the figure legend, the  $x$ - or  $y$ -label indicates the scattering amplitude if the incident light is  $x$ - or  $y$ -polarized. The number corresponds to the size parameter of the given calculation. This plot corresponds quite nicely to BH's figure 13.2, if we let the  $x$ -components correspond to BH's parallel components.

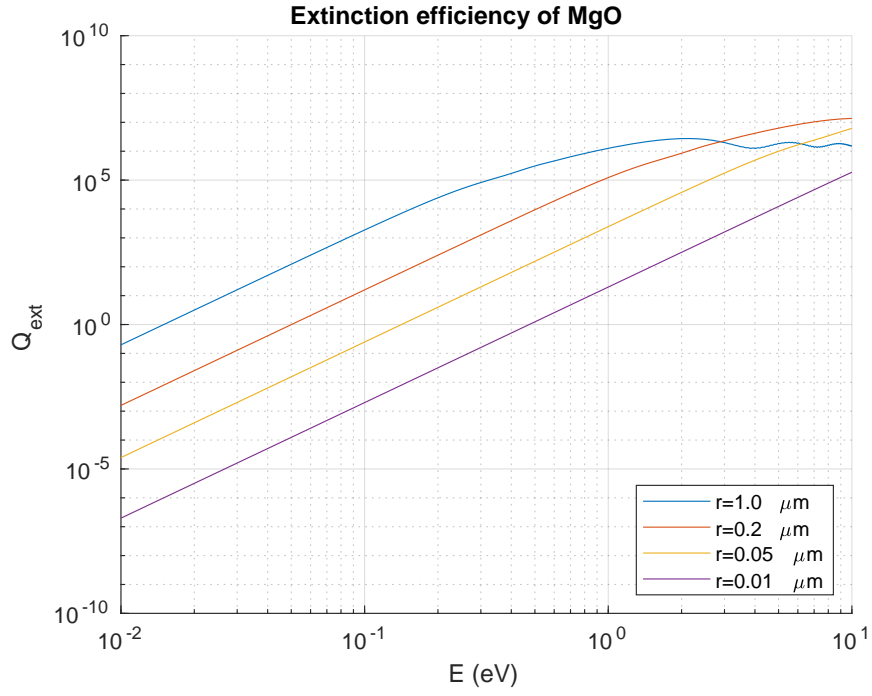


Figure 5: The extinction efficiency of MgO as a function of photon energy.

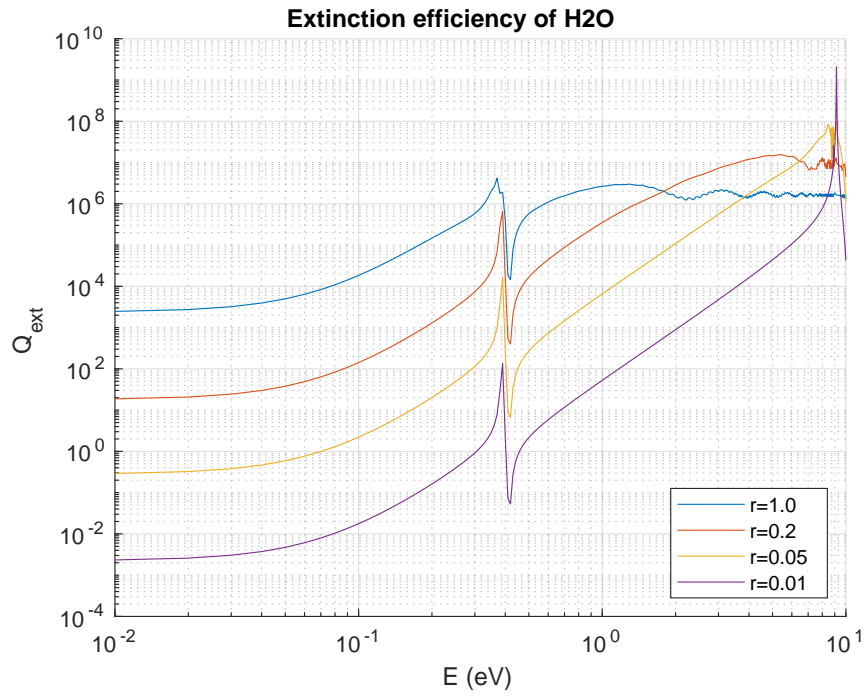


Figure 6: The extinction efficiency of water as a function of photon energy.

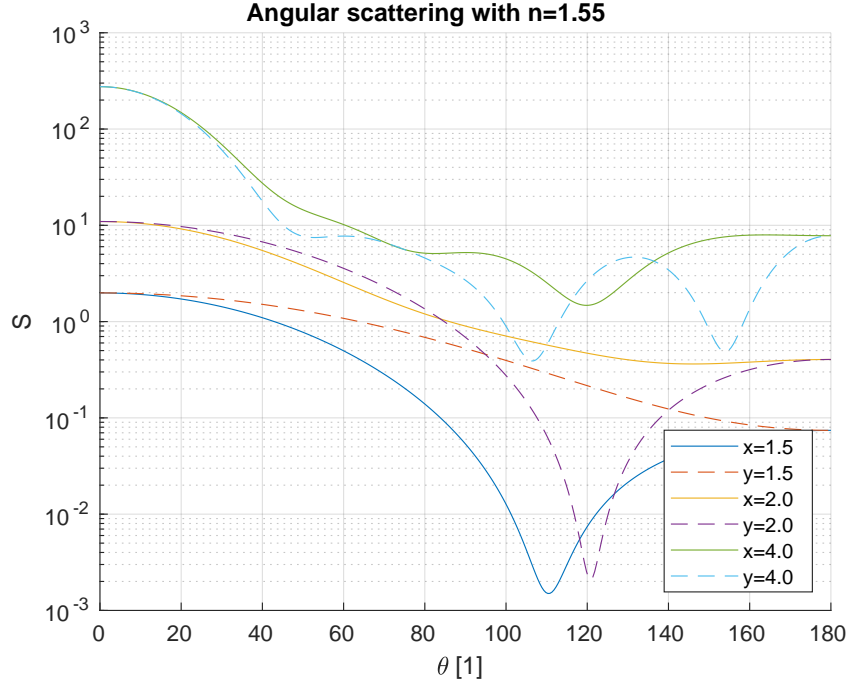


Figure 7: The absolute value of the perpendicular and parallel polarization components of the scattering matrix, plotted over different scattering angles for a few different size parameters.

## 5 Scattering cross section and extinction efficiency for Ag and Au in air and SiO<sub>2</sub>

Mainly, the exact same approach is used here. The quantities  $C_{\text{sca}}$  and  $C_{\text{ext}}$  are sought from the Mie calculation, and the extinction cross section is divided by the cross sectional area. The refractive index of Ag and Au are calculated from the Drude model, with parameters looked up in [4]. Three different particle radii are shown,  $a = \lambda_{\text{min}}/10000$ ,  $a = \lambda_{\text{min}}/100$  and  $a = \lambda_{\text{min}}$ , ranging from well below the quasistatic limit to being certainly above. The plots of these are shown in figs. 8 to 11.

The quasi-static approximate solution is plotted in Maier[3] fig. 5.3. It seems to be anchored in a completely different regime on the y-axis (are those astronomical units??). The Mie theory calculations are missing the sharp peak, which arose from the properties of the dielectric function allowing the denominator in Maier eq. (5.14) to become zero.

## References

- [1] ALLARDICE, J., AND LE RU, E. Convergence of mie theory series: criteria for far-field and near-field properties. *Applied Optics* 53 (11 2014).
- [2] BOHREN, C. F., AND HUFFMAN, D. R. *Absorption and Scattering of Light by Small Particles*. Wiley-VCH Verlag GmbH & Co. KGaA, 2004. (reprint).
- [3] MAIER, S. A. *Plasmonics: Fundamentals and Application*. Springer, 2007.
- [4] MOROZ, A. <http://www.wave-scattering.com/drudefit.html>, 2019. Accessed: 2020-04-30.

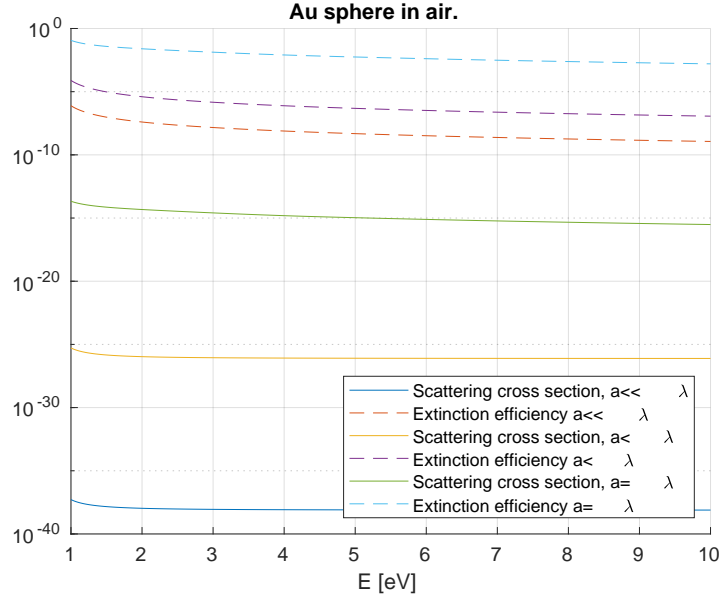


Figure 8: Scattering cross sections and extinction efficiencies of an Au sphere in air, for three different particle sizes, ranging from 1/10000 of the shortest wavelength to equaling the shortest wavelength, as a function of incoming photon energy.

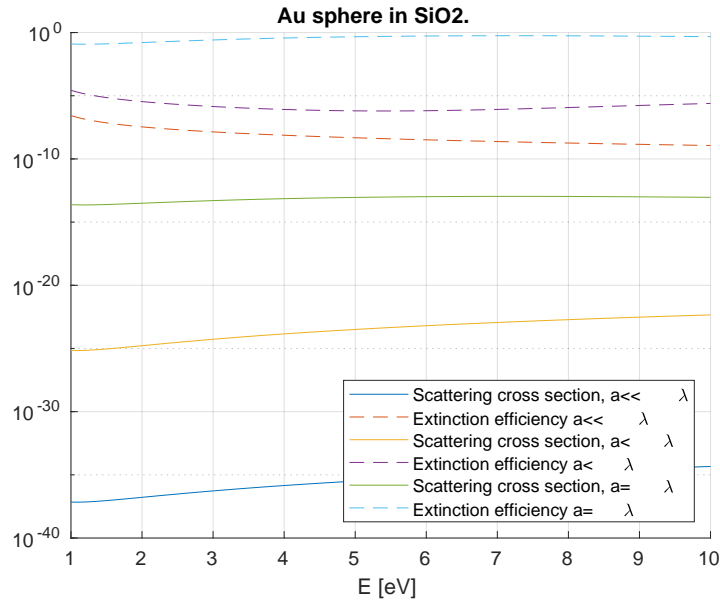


Figure 9: Scattering cross sections and extinction efficiencies of an Au sphere in SiO<sub>2</sub>, for three different particle sizes, ranging from 1/10000 of the shortest wavelength to equaling the shortest wavelength, as a function of incoming photon energy.



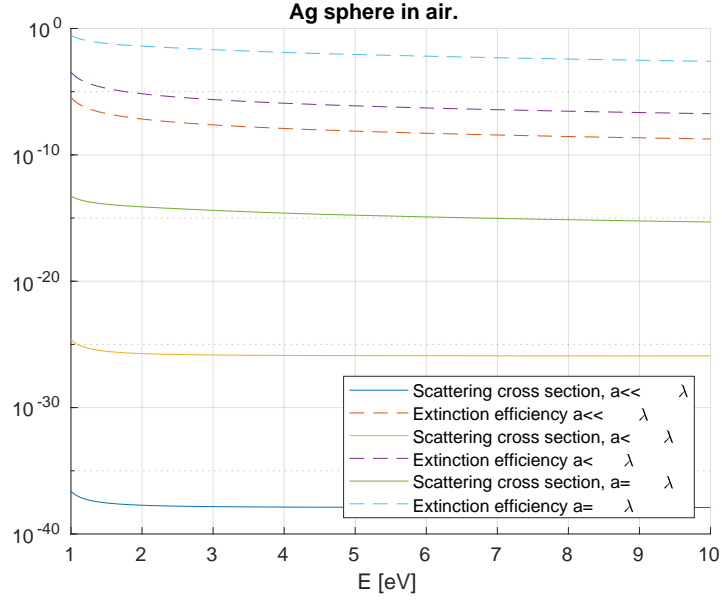


Figure 10: Scattering cross sections and extinction efficiencies of an Ag sphere in air, for three different particle sizes, ranging from 1/10000 of the shortest wavelength to equaling the shortest wavelength, as a function of incoming photon energy.

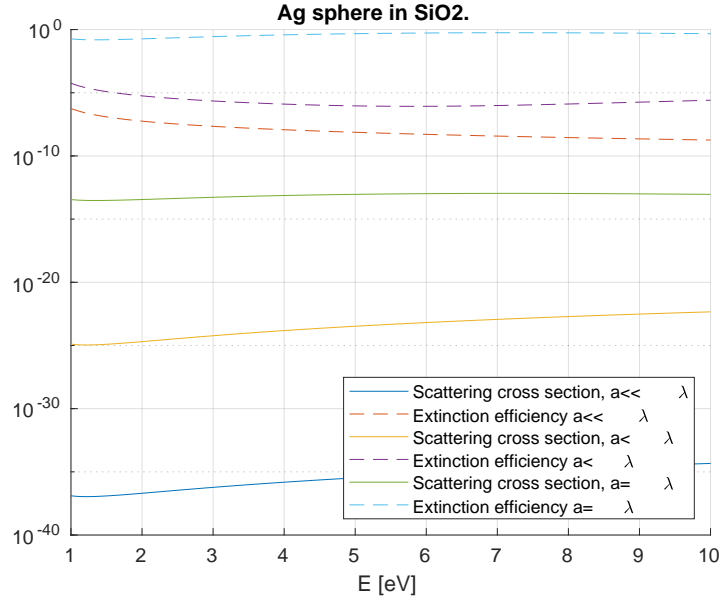


Figure 11: Scattering cross sections and extinction efficiencies of an Ag sphere in SiO<sub>2</sub>, for three different particle sizes, ranging from 1/10000 of the shortest wavelength to equaling the shortest wavelength, as a function of incoming photon energy.

- [5] STEPHENS, R. E., AND MALITSON, I. H. Index of refraction of magnesium oxide. *Journal of Research of the National Bureau of Standards* 49, 4 (10 1952), 249 – 252.
- [6] THE INTERNATIONAL ASSOCIATION FOR THE PROPERTIES OF WATER AND STEAM. Release on the refractive index of ordinary water substance as a function of wavelength, temperature and pressure. <http://www.iapws.org/relguide/rindex.pdf>, 1997.
- [7] WISCOMBE, W. J. Improved mie scattering algorithms. *Applied Optics* 19 (1980), 1505 – 1509.